

SIZE AND MORPHOLOGY OF PARTICLES GENERATED BY SPRAYING POLYMER-MELTS WITH CARBON DIOXIDE

P. Kappler*¹, W. Leiner¹, M. Petermann², E. Weidner¹

¹ University Bochum, Process Technology, 44780 Bochum, Germany

E-mail: weidner@vtp.ruhr-uni-bochum.de, Fax: +49 234 32 14277

² University Bochum, Particle Technology, 44780 Bochum, Germany

INTRODUCTION

Powder generation by spray processes that make use of the unique properties of supercritical fluids opens new ways to manufacture particles with tailor-made properties. Therefore the knowledge of the interdependencies between process conditions and size/morphology of the particles is essential. By statistical evaluation of an experimental study for powder generation from polyethyleneglycol (6000 g/mol) by the PGSSTM - process (Particles from Gas Saturated Solutions) correlations were developed, that allow to model particle size, morphology and bulk density from process conditions (pressure, temperatures, flow rates). The experiments were performed on a new type of continuously operated pilot plant with a capacity of 50 kg/h of powder. Spheres, porous spheres, porous irregular particles, micro-foams and fibres were generated in sizes from the low micrometer range up to some hundred micrometers. Bulk densities of the powders are between 90 kg/m³ and 600 kg/m³.

The mechanisms of powder generation in an expanding jet of a mixture of gas and molten polymer are identified and quantified. Calculations on heat conductivity, heat transfer, solidification resp. crystallisation, nucleation and growth of gas bubbles indicate, that the morphology is controlled by different mechanisms depending on the size of the particles [1].

EXPERIMENTAL SECTION AND SUBSTANCES

A new continuously operated PGSS-plant was built to maintain stationary process conditions in a technical sized process. Therefore the plant was designed for a capacity up to 50 kg powder generation per hour. Typical spraying times at stationary conditions were from some minutes to hours. The plant was constructed for pressures up to 350 bar at a maximum temperature of 200 °C. An computerized measurement system is used to control and visualize the experiments and to store the experimental data for post process calculations [2, 3].

The system PEG-6000 - CO₂ was chosen as a model system. Polyethyleneglycols (PEGs) are ingredients of many life science and pharmaceutical products. Pure PEG-6000 melts at about 60 °C and the viscosity of the molten PEG-6000 lies between 1200 mPas (at 60 °C) and 400 mPas (at 100 °C). With dissolved CO₂ the viscosity of PEG-6000 can be reduced to 200 mPas at saturation pressures of 200 bar [4, 5].

EXPERIMENTS AND RESULTS

The plant described above was used to carry out more than 200 experiments with PEG-6000. Aim was to determine the dependencies of particle properties on the process conditions. Spraying pressure and temperature as well as the gas to product ratio GTP (CO₂ mass flow/polymer mass flow) were identified as main process parameters. Based on the obtained experimental data, regression functions were derived to characterise the dependencies between the particle properties and the process conditions.

To describe the morphology of the particles mathematically a so-called morphology coefficient was defined. For each characteristic shape of the obtained particles a discrete number was introduced (see **table 1**).


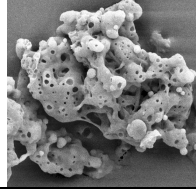
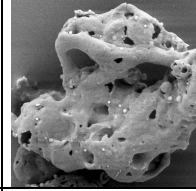
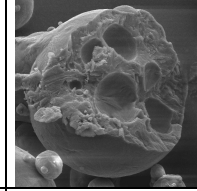
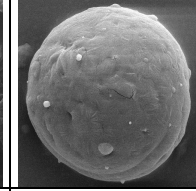
morphology coefficient F	0,2	0,4	0,6	0,8	1
					
particle shape	fibres	micro-foams	porous irregular particles	porous spheres	spheres

Table 1: **morphology coefficient F**

Thus for each particle property (average diameter $d_{p0,5}$, morphology coefficient F and bulk density ρ_b) a regression function with the variables spraying pressure p, pre-expansion temperature T and the gas to product ratio (GTP) was obtained:

$$\text{average diameter } (d_{p0,5} / \mu\text{m}) = 1,4 \cdot 10^{-6} \frac{(T / \text{K})^{3,088}}{(p / \text{bar})^{0,125} \cdot \text{GTP}^{0,367}} \quad (\text{relative error} = 22 \%), \quad (1)$$

$$\text{morphology coefficient } F = 6,9 \cdot 10^{-11} \frac{(T / \text{K})^{4,247}}{(p / \text{bar})^{0,403} \cdot \text{GTP}^{0,105}} \quad (\text{relative error} = 14 \%), \quad (2)$$

$$\text{bulk density } (\rho_b / (\text{g} / \text{ml})) = 5,2 \cdot 10^{-17} \frac{(T / \text{K})^{6,574}}{(p / \text{bar})^{0,552} \cdot \text{GTP}^{0,106}} \quad (\text{relative error} = 15\%), \quad (3)$$

equations (1) to (3) are valid for: $323 \text{ K} < T < 373 \text{ K}$; $50 \text{ bar} < p < 350 \text{ bar}$; $0,1 < \text{GTP} < 10$

A plot of equation (1) at a constant temperature of $T = 80 \text{ }^\circ\text{C}$ is shown in **Figure 1**. The average diameter $d_{p0,5}$ decreases with increasing spraying pressure p and rising GTP. At GTP below 4, the particle size depends strongly on the ratio between gas and polymer, while at higher GTP the influence is less pronounced. An initial amount of gas is required, to establish a spray and to generate small particles. A further increase of the gas throughput (at constant polymer flow) does not contribute much to the generation of new surfaces and thus to the formation of smaller particles.

The results in **Figure 1** are valid for one specific pre-expansion temperature. If the temperature is increased, the average diameter $d_{p0,5}$ raises and a new surface above that one shown in **Figure 1** would describe the experimental results. The solutions of the equations (2) and (3) can be diagrammed equivalent to the solution of equation (1) [1].

One aim of this research project was to identify operating conditions for the PGSS-process to generate particles with defined properties. This includes the particle size as well as the morphology of the particles.

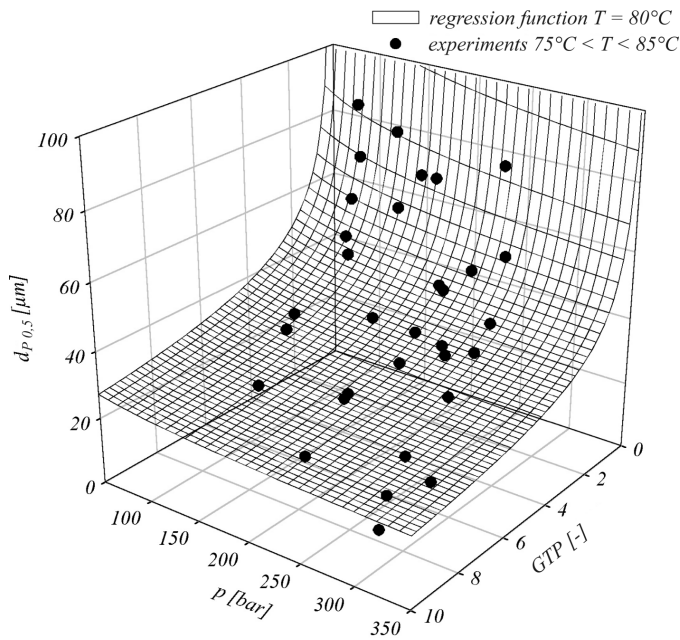


Figure 1: regression function and experimental data for $d_{p,0.5}$ at a constant temperature $T = 80^\circ\text{C}$

Therefore the equations shown above were used to form a three-dimensional plot which characterises regions of different morphology and different particle size. In addition regions with different bulk densities, another important parameter for powderous products, are shown in this diagram. A cut of this diagram at a constant gas to product ratio $GTP = 1$ is illustrated in **Figure 2**. To produce PEG-6000 particles with tailor made properties, the required process parameters can be taken from this diagram.

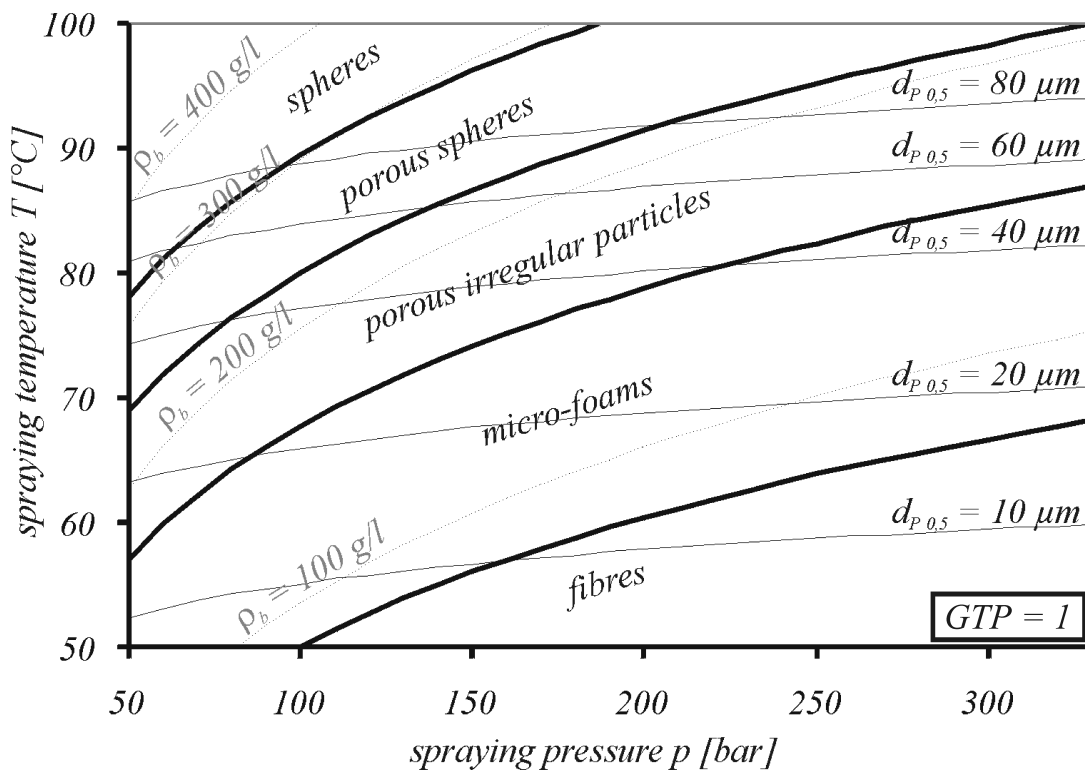


Figure 2: curves of constant average diameter $d_{p,0.5}$ and bulk density ρ_s and areas of constant morphology (index F) in dependence of spraying pressure p and pre-expansion temperature T at a gas to product ratio $GTP = 1$

As an example, **Figure 2** shows that at a constant gas to product ratio $GTP = 1$, particles with an average diameter $d_{p,0.5} = 40 \mu\text{m}$ can be produced at $p = 300 \text{ bar}$ and $T = 80^\circ\text{C}$, $p = 150 \text{ bar}$

and $T = 78\text{ }^\circ\text{C}$ or at $p = 60\text{ bar}$ and $T = 75\text{ }^\circ\text{C}$. If the areas of particle morphologies are considered, it is obvious that although the particles have the same size, the morphologies differ considerably. For the first example ($p = 300\text{ bar}$ and $T = 80\text{ }^\circ\text{C}$) micro-foams are produced, for the second set of conditions irregular particles and for the third one porous spheres are generated. The bulk density of powders is directly coupled to the morphology of the single particles. Therefore it is not surprising that the slope of the curves of constant bulk density ρ_S is similar to those of constant morphology coefficients F .

CALCULATIONS

Impulse and heat transfer

Basic impulse, heat and mass transfer mechanisms were investigated to understand the physical phenomena that lead to the observed influences of the process parameters on the particle properties. As a first approach, estimations of impulse, heat and mass transfer between the polymer droplets and the expanding CO_2 in the spraying tower gave information about the different mechanisms, like heat conduction and heat transfer, deceleration of the droplets and crystallisation. To identify which mechanism dominates the powder formation, characteristic times were defined as followed:

- characteristic flight duration: duration of the deceleration until stationary sink rate of the particle is reached
- characteristic duration of heat transfer: duration of cooling until the particle surface reaches solidification temperature
- characteristic duration of heat conduction: duration of cooling until the particle centre reaches solidification temperature
- characteristic duration of crystallisation: duration until complete crystallisation of the particle

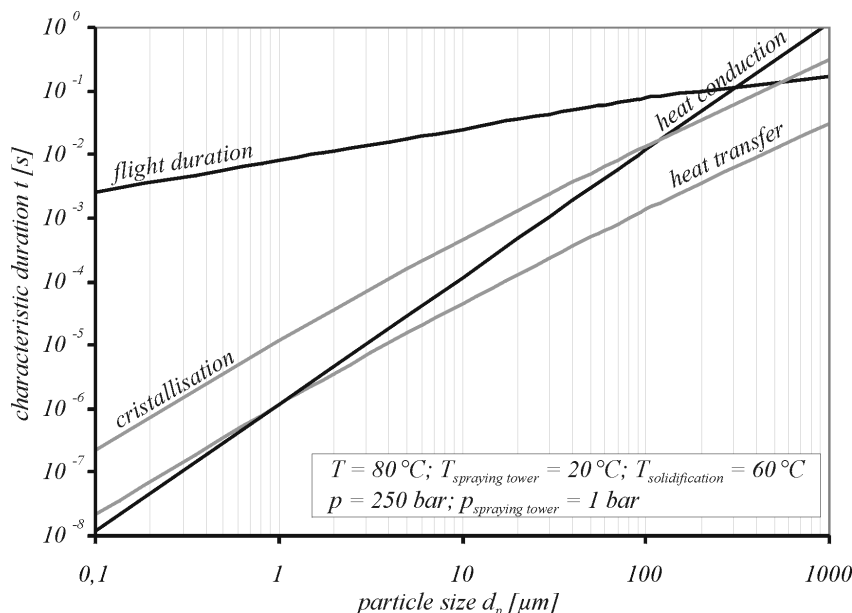


Figure 3: characteristic durations of the particle formation mechanisms as a function of the particle size d_p at constant spraying pressure and temperature

The different mechanisms mainly depend on particle size (**Figure 3**), temperature and pressure. The characteristic flight duration can be interpreted as the minimum residence time the particles should have in the spraying tower, before they reach a solid wall.

All the characteristic times are shorter than the characteristic flight duration except for $d_p > 300\text{ }\mu\text{m}$, which means that the solidification of small particles is fast enough to be completed during their flight path in the tower.

For particles bigger than 100 μm the characteristic duration of the heat transfer is one order lower than that of heat conduction, which means that the heat contained in the particle is very quickly transferred into the surrounding expanding gas. Therefore the surface of the particle is cooled down, while in the center the temperatures still are high. Resultant the complete solidification of the particles is delayed, which supports the formation of sealed surfaces and spherical particles. If d_p is bigger than 130 μm the characteristic duration of crystallization is less than the duration of heat conduction. This leads probably to crystallization of the particle surface, while the centre of the particle is still liquid.

Bubble growth

To describe the particle formation during the expansion step of the PGSS-process, the degassing of the admixed and dissolved CO_2 has to be taken into account. In combination with the heat transfer effects shown above, a model for the different morphologies, obtained in the spray experiments, was developed. During expansion bubbles can either be formed by homogeneous nucleation or by mechanically dispersed gas. For bubbles formed by homogeneous nucleation, the initial radius is calculated based on Becker and Döhning [7]. While expanding from pre-expansion conditions to spraying-tower conditions the radius of CO_2 bubbles may increase by a factor of ten or even more due to the density decrease [1]. If surplus CO_2 is present the initial radius of the bubbles can be estimated through the final bubble radius as seen on the REM-pictures of broken porous particles, by assuming a radius increase during the expansion of 10. The bubble growth based on Leiner [8] was calculated, as given in equation (4):

$$p_v - p_{L\infty} = (\rho_L - \rho_v) r_B \cdot r_B'' + \frac{\varepsilon}{2} (3\rho_L - \rho_v) r_B'^2 + 4\eta_L \varepsilon \frac{r_B'}{r_B} + \frac{2\sigma_{LV}}{r_B}, \quad \text{with} \quad \varepsilon = \frac{\rho_L - \rho_v}{\rho_L}. \quad (4)$$

SUMMARY AND CONCLUSIONS

Various particle sizes, shapes and bulk densities were produced with a new continuously operated PGSS-plant. From experimental data, correlations between process conditions and particle properties were derived. Applying these functions allow to identify process parameters to produce PEG-6000 particles with tailor made properties.

Mechanisms of PGSS powder generation were estimated by calculations on heat conductivity, heat transfer, crystallisation, nucleation and growth of gas bubbles. The particle formation mainly depends on particle diameter, pre- and postexpansion temperature and spraying pressure. Based on the experimental observations, statistical evaluation and the assumed transfer mechanisms a first model of particle formation by spraying polymer-melts with supercritical fluids could be developed. On the example of the formation of microfoam and porous particles, the model is illustrated in **Figure 4**.

Immediately after the mixture of polymer and CO_2 leaves the nozzle as spray, CO_2 bubbles in the droplets grow exponentially against the viscosity forces and inertia forces of the surrounding polymer until a constant growth velocity is reached after approximately 10^{-8} s to 10^{-7} s, depending on the process conditions. In the case of $T = 100^\circ\text{C}$ and $p = 100$ bar (left side in **Figure 4**) the particle surface solidifies after approximately 10^{-4} s, because the rate of crystallization is faster than the heat conduction. The centre of the particle is liquid. Gas bubbles still are included in the liquid. Due to the high viscosity of the liquid polymer, the bubbles are entrapped and cannot penetrate the solid surface. After 10^{-2} s the particle is completely solidified.

At pre-expansion conditions of $T = 80^\circ\text{C}$ and $p = 250$ bar (right side in **Figure 4**) more CO_2 is dissolved in the polymer and the bubble growth is accelerated. Due to the high pressure

difference, the temperature in the bubbles sinks very fast. The bubble surfaces may solidify while the surrounding particle is still liquid. If the bubbles are not completely depressurised, till the walls solidify, the bubbles will probably decompress by perforating the particle surfaces. Sponge-like microfoams are formed. After 10^{-4} s the particle solidifies instantly because there is no distinct temperature gradient in the particles left.

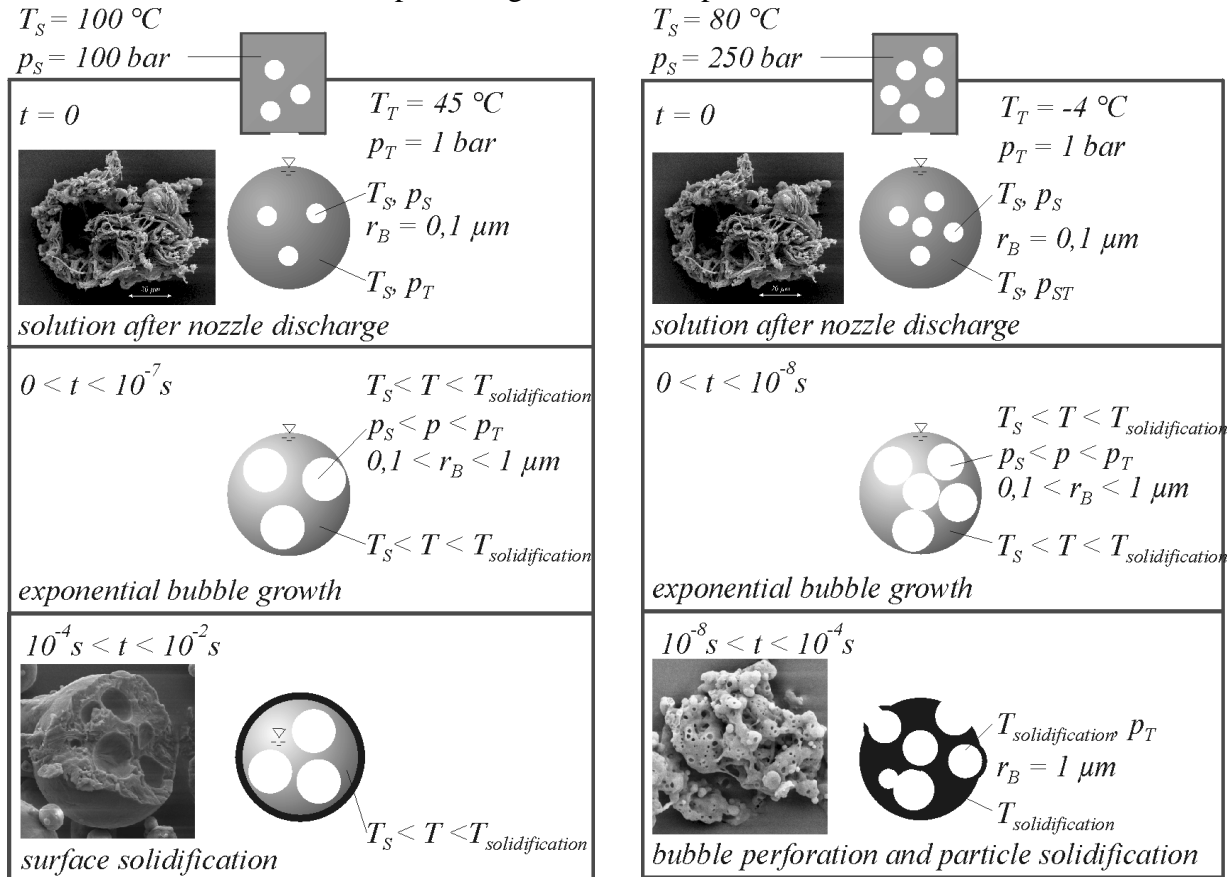


Figure 4: model of particle formation for porous spheres (left side) and micro-foams (right side) index S = pre-expansion conditions, index T = spraying tower conditions

ACKNOWLEDGEMENTS

The authors like to thank Hydro Gas and Clariant for supplying the CO₂ resp. PEG.

REFERENCES

- [1] Kappler, P., Partikelbildung und Morphologie bei der Hochdruckmikronisierung gashaltiger Lösungen, PhD thesis, Ruhr University, Bochum, **2002**, in press
- [2] Weidner E., Powderous composites by high pressure spray processes, Proc. 6th Int Symp on supercrit fluids, 28 – 30 April 2003, Versailles, in press
- [3] Weidner, E., Knez, Z., Precipitation of solids with dense gases, High Pressure Process Technology: Fundamentals and Applications, Bertuccio, A., Vetter, G.(Eds.); Elsevier, **2001**
- [4] Kukova, E., Phasenverhalten und Transporteigenschaften binärer Systeme aus Polyethylenglykolen und Kohlendioxid, PhD thesis, Ruhr University, Bochum, **2002**, in press
- [5] Kukova, E., Petermann, M., Weidner, E., Phase behavior (s-l-g) and fluiddynamic properties of high viscous polyethyleneglycols in the presence of compressed carbondioxide, Proc. 6th Int Symp on supercrit fluids, 28 – 30 April 2003, Versailles, in press
- [6] Becker, R., Döhring, W., Kinetik der Keimbildung in überhitzten Dämpfen, Ann. Phys. 24, **1935**
- [7] Leiner, W., Wärmeübergang und Blasenbildung beim Behältersieden, Deutscher Universitätsverlag, Wiesbaden, **1990**